

## Measuring Interfacial Tension Between Oil and Nano-Saline Solutions in the Presence of SiO<sub>2</sub> or TiO<sub>2</sub> at Low and Intermediate Pressures

M. Noor Ghasemi<sup>a</sup>, S. Heidari<sup>a</sup>, Sh. Ramezanzadeh<sup>a</sup>, G.R. Vakili-Nezhaad<sup>b</sup> and F. Esmailzadeh<sup>a,\*</sup>

<sup>a</sup>Department of Chemical and Petroleum Engineering, School of Chemical and Petroleum Engineering, Enhanced Oil and Gas Recovery Institute, Advanced Research Group for Gas Condensate Recovery, Shiraz University, Shiraz, Iran, 7134851154

<sup>b</sup>Petroleum and Chemical Engineering Department, College of Engineering, Sultan Qaboos University, Muscat 123, Oman

(Received 17 June 2021, Accepted 24 September 2021)

In this paper, SiO<sub>2</sub> and/or TiO<sub>2</sub> nanoparticles (NPs) were used to enhance the performance of water injection process causing an increase in oil recovery. To this end, several nano saline solutions were prepared from each of the following salt compounds: NaCl, CaSO<sub>4</sub>, or MgSO<sub>4</sub> (1000 ppm) together with different concentrations of SiO<sub>2</sub> and/or TiO<sub>2</sub> NPs from 0.01 to 0.07 wt.%. Interfacial tensions (IFT) between the oil, collected from Sarvestan oil reservoir, and the saline solutions were measured at low and intermediate pressures, *i.e.* 14.5, 72.5, 145, 217.5, 290, 362.5, 435, 507.5, and 1160 Psi using a homemade IFT-device. Results showed that SiO<sub>2</sub> and/or TiO<sub>2</sub> NPs successfully reduced the interfacial tension between the oil and the saline solutions. The maximum reductions of 63.95% and 63.46% were obtained at the pressure of 507.5 Psi for 0.05 wt.% of SiO<sub>2</sub> in the MgSO<sub>4</sub>-H<sub>2</sub>O solution and 0.05 wt.% of TiO<sub>2</sub> in the CaSO<sub>4</sub>-H<sub>2</sub>O solution, respectively. The maximum IFT reductions for NaCl-H<sub>2</sub>O-TiO<sub>2</sub>, NaCl-H<sub>2</sub>O-SiO<sub>2</sub>, MgSO<sub>4</sub>-H<sub>2</sub>O-TiO<sub>2</sub>, and CaSO<sub>4</sub>-H<sub>2</sub>O-SiO<sub>2</sub> solutions were 58.13%, 49.65%, 36.18%, and 20.88%, respectively.

**Keywords:** Interfacial tension, SiO<sub>2</sub> nanoparticles, TiO<sub>2</sub> nanoparticles, Enhanced oil recovery, Wettability

### INTRODUCTION

Enhanced oil recovery (EOR) methods are generally classified into three groups: chemical, thermal, and miscible recovery methods. Chemical methods generally decrease the oil viscosity, interfacial tension (IFT), and wettability. In thermal methods, the oil recovery factor increases as a result of an increase in the oil thermal expansion. In miscible methods, miscible gases decrease the oil viscosity, and therefore, increase the oil recovery factor [1].

Nanoparticles with the ability of developing oil and gas industries can be used for several purposes including exploration, drilling, production, and recovery. Nanoparticles contribute to efficient, cheap, and eco-friendly technologies [1-3]. The idea of using nanoparticles

in EOR methods has been recently introduced by several researchers [4-7]. Kong *et al.* examined nano and micro technologies for the oil and gas industries [8]. Fangda *et al.* used nanoparticles for a surfactant flooding process and searched the optimum conditions of the nano-surfactant emulsion. Results confirmed that the optimum conditions were vastly sensitive to the thermal recovery process [9]. Elkady *et al.* increased oil recovery factor up to 67.16% through nano-polymer flooding [1]. Biyouki *et al.* examined IFT reduction between the oil and water by synthesizing nickel oxide NPs using two different methods: in-situ combustion (ISC) and ex-situ combustion (ESC). In the ISC method, the nickel aqueous solution was dispersed in the heavy oil solution (prepared from asphaltene, toluene, and gasoil) in a Parr reactor unit at certain temperature and pressure. However, a simple precipitation method was implemented in the method of ESC. Additionally, NiO NPs synthesized by the ISC method tend to form more coke

\*Corresponding author. E-mail: [esmaeilzadeh95@gmail.com](mailto:esmaeilzadeh95@gmail.com)

deposition compared to those synthesized by the ESC method [10]. According to Eq. (1), a decrease in interfacial tension causes an increase in the capillary number, and hence enhances the oil recovery factor [7].

$$N_c = G \frac{v\mu}{\delta} \quad (1)$$

where  $N_c$ ,  $v$ ,  $\mu$  and  $\delta$  are the capillary number, Darcy velocity, viscosity of displacing fluid, and the interfacial tension, respectively.

Ranjbar *et al.* assessed the influence of  $\gamma$ -Al<sub>2</sub>O<sub>3</sub> and MgO NPs on the surface tension and concluded that there is not a certain amount of NPs concentration, which can be considered as an optimum value to reduce surface tension [11]. Amraei *et al.* used a nanofluid including SiO<sub>2</sub> NPs, Span-80, Tween-80, (CTAB), (SDS), Lauric alcohol-3EO, and K-Laurate surfactants in water and subsequently examined the impact of temperature on reduction of the IFT between the oil and water. Their findings revealed that increasing the temperature led to a decrease in IFT between the oil and water [12]. Ziad *et al.* evaluated the role of morphology of aluminum oxide NPs on the reduction of oil IFT. Results showed that changing morphology improved the dispersion of NPs and consequently, increased oil recovery [13].

Although there are many research on the effect of NPs on decreasing IFT, to the best of our knowledge, our work is the first study that examines the impact of SiO<sub>2</sub> and/or TiO<sub>2</sub> NPs on IFT reduction between the oil and Asaline solutions at low and intermediate pressures. As expected, low saline solutions increase oil recovery to an acceptable level [14]. Furthermore, recent researches have shown that adding NPs to saline solutions can promote more desirable reduction of IFT between the saline solution and oil [10,13-17]. Therefore, both low saline solutions and NPs were used in this study to reduce IFT between the oil and saline solutions. In addition, several saline solutions were first prepared from NaCl, CaSO<sub>4</sub>, and MgSO<sub>4</sub> salts. Then, SiO<sub>2</sub> and/or TiO<sub>2</sub> NPs were separately dispersed into the saline solutions by a sonicating device. Finally, IFT between the oil and saline solutions was measured using a homemade IFT device under low and intermediate pressures.

## MATERIALS AND INSTRUMENTS

Sodium chloride (NaCl, 99 wt.%), calcium sulfate (CaSO<sub>4</sub>, 99 wt.%) and magnesium sulfate (MgSO<sub>4</sub>, 99 wt.%) were provided from Sigma-Aldrich Chemical Company (Milwaukee, WI) and exploited for the preparation of saline solutions. Silica oxide chemical compound (SiO<sub>2</sub>, particle size range of 20-30 nm, true material density of 3.4 g cm<sup>-3</sup>, specific surface area between 180-600 m<sup>2</sup> g<sup>-1</sup>, Merck Company) and titanium dioxide chemical compound (TiO<sub>2</sub>, particle size range of 20-30 nm, true material density of 3.9 g cm<sup>-3</sup>, specific surface area between 200-240 m<sup>2</sup> g<sup>-1</sup>, Merck Company) were used as the nanoparticles. Table 1 shows the NPs characteristics. Distilled water was used as solvent to prepare the solutions. Oil sample with a density of 90 g ml<sup>-1</sup> and viscosity of 39 cP was supplied from Sarvestan oil-reservoir located in south of Iran. A probe-type sonication (Tomy, UD-201, Japan) was employed to disperse NPs into the saline solutions. A Haskel pump (3L SS-41-H) was used to pressurize samples in the IFT device. The digital balance (Sartorius balance, BP 210 S, German) was measured the weight of salt samples. A digital microscopic camera (Dino-Lite Digital Microscope, Maximum magnification of 220, Taiwan) was utilized to record pictures of appeared bubbles in the IFT device.

A high-pressure and temperature IFT device (Fig. 1) at the Oil and Gas Thermodynamic Laboratory, Shiraz University was calibrated by carbon dioxide-water system and exploited to measure IFT values between Sarvestan oil and saline solutions containing NPs. A detailed explanation of the IFT device has been reported in our previous work [18].

## EXPERIMENTS

Saline solution samples (1000 ppm) were prepared from each of these salt compounds: NaCl or CaSO<sub>4</sub> or MgSO<sub>4</sub>. Also, it should be noted that increasing brine salinity causes the agglomeration of NPs due to reduction of the Zeta potential [19]. The concentrations of brines was considered 1000 ppm in this study. SiO<sub>2</sub> and/or TiO<sub>2</sub> NPs were separately added to the saline solutions to prepare saline solutions containing NPs with the concentrations of 0.01, 0.03, 0.05, and 0.07 wt.%. The NPs were then sonicated

**Table 1.** The Characteristics of NPs

Nanoparticle	Particle size range (nm)	True material density (g cm <sup>-3</sup> )	Specific surface area (m <sup>2</sup> g <sup>-1</sup> )
SiO <sub>2</sub>	20-30	3.4	180-600
TiO <sub>2</sub>	20-30	3.9	200-240

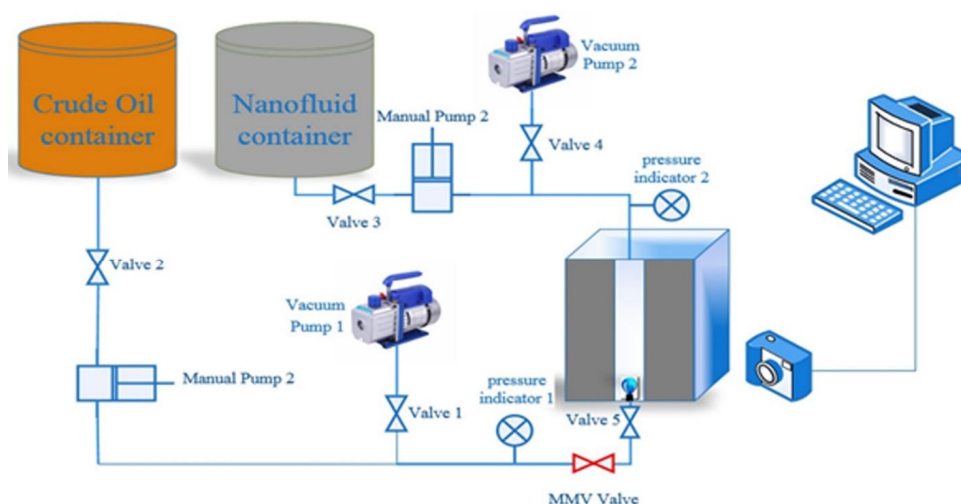


**Fig. 1.** Schematic diagram of the homemade high-pressure and temperature IFT device.

(100 kHz) for 20 min to adequately disperse them in the saline solution. All the tests were carried out at ambient temperature (25 °C). It is expected that surface tension decreases at higher temperatures, due to reduction of molecular interactions between NPs and rock reservoir.

The accuracy of the IFT device was first checked by carbon dioxide-water system and compared to the experimental data reported in the published literature. To do so, the container was filled with double-distilled water. The surface tension of distilled water at the temperature of 25 °C was measured at different pressures, *i.e.* 72.5, 217.5, 362.5, 507.5, and 580 psia. To this end, a gas bubble was produced at the bottom section of the device at each pressure. The camera was recorded several pictures of the bubble growing into the fluid container. The largest length and width of the bubble, which are on the verge of separation from the ostium, were recorded to calculate the correction factor needed for the IFT measurement. Figure 2

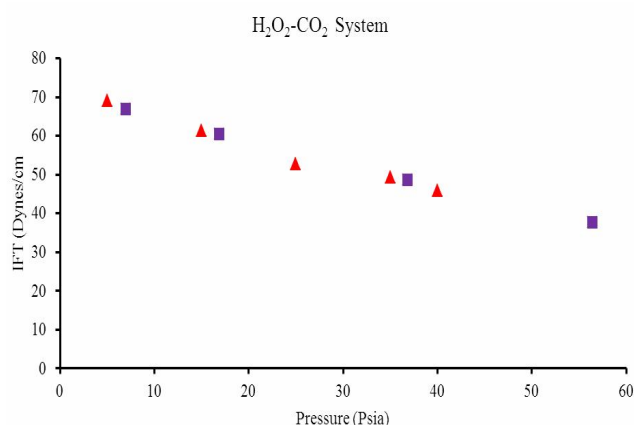


**Fig. 2.** Water surface tension in carbon dioxide-water system at 25 °C.

shows the experimented results of water-CO<sub>2</sub> surface tension obtained in this work that is compared to those

reported in the literature. As can be seen, the experimental results of this work were in line with those published in the literature with an average absolute relative deviation (AARD%) of less than 5% [20].

After calibrating the IFT device, the IFT between the oil and different nano saline solutions was measured by filling the container with a certain amount of brine. The oil was pressurized using a Haskel pump. It was then injected into the brine solution as a small drop using a tiny needle at the desired pressure. The digital camera continually recorded the images of the oil drop in the brine, as shown in Fig. 3. Finally, the container was depleted, and this method was repeated for all nano-saline solutions at various concentrations and pressures. The IFT values between the oil and brine were calculated by analyzing the prepared images.

In this study, Andreas empirical relationship [21], Eq. (2), was used to calculate oil interfacial tension.

$$\delta = \frac{g D_e^2 \Delta\rho}{H} \quad (2)$$

where  $\delta$ ,  $\Delta\rho$ ,  $D_e$ , and  $H$  are the interfacial tension, density difference between fluids, the highest diameter of the bubble width, and the correction factor, respectively. The correction factor,  $H$ , could be calculated from Eq. (3).

$$S = \frac{D_s}{D_e} \quad (3)$$

where  $D_s$  and  $D_e$  are the highest width and highest length of the bubble, respectively.

## RESULTS AND DISCUSSION

In this study, oil interfacial tension was measured in of the presence of saline solutions (NaCl, CaSO<sub>4</sub>, MgSO<sub>4</sub>, 1000 ppm) containing various weight percentages of SiO<sub>2</sub> and/or TiO<sub>2</sub> NPs (0.01, 0.03, 0.05 and 0.07 wt.%) at different pressures of 15, 73, 145, 218, 290, 363, 435, 508, and 1160 Psi, and at ambient temperature (25 °C).

The obtained interfacial tensions between the oil and NaCl-H<sub>2</sub>O solutions (1000 ppm) containing 0.01, 0.03, 0.05, and 0.07 wt.% of SiO<sub>2</sub> NPs and 0.01, 0.03, 0.05 of TiO<sub>2</sub>



**Fig. 3.** An image of the oil drop in the high-pressure IFT device.

NPs are shown in Fig. 4 (a and b). As can be seen, the interfacial tension decreased up to 0.05 wt.% with an increase in concentration of NPs. This is due to increase of Brownian motion resulting from repulsion forces. Increasing the NPs can significantly alter wettability; this indicates that the texture and porosity of the reservoir rock can be modified and improved in the presence of NPs. On the other hand, based on the Zeta potential analysis shown in Table 2, SiO<sub>2</sub> nano-saline solution at the concentration of 0.07 wt.% has lower effect on increasing the IFT compared to that at concentration of 0.05 wt.%; this is due to the coagulation and agglomeration phenomena [7,22-24]. In addition, increasing the pressure caused a decrease in the interfacial tension between the oil and the NaCl-H<sub>2</sub>O-SiO<sub>2</sub> solutions. The descending trend of the IFT reduction was continued even at intermediate pressures. Although the changes in IFT were negligible after 600 Psi, the results confirmed that the pressure was a vital factor on the IFT reduction. Therefore, the addition of SiO<sub>2</sub> and/or TiO<sub>2</sub> NPs into the NaCl-H<sub>2</sub>O solutions improved the oil recovery factor, especially at intermediate pressures.

Table 2 shows the results of Zeta potential analysis after the end of each experiment for nano-saline solutions containing 0.05-0.07 wt.% of SiO<sub>2</sub> NPs and 0.05 wt.% of TiO<sub>2</sub> NPs. To do so, a specific amount of nanofluids with different concentration of nanoparticles was separated and

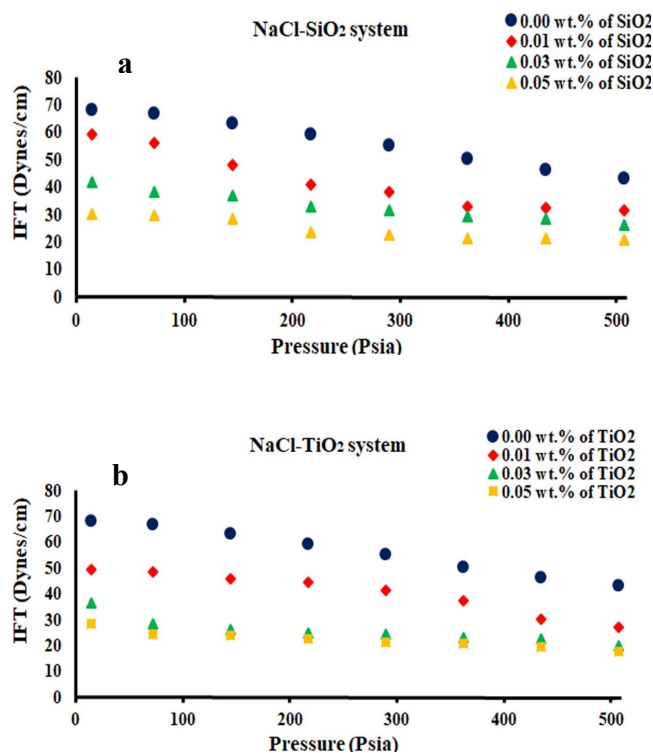


**Fig. 4.** Experimental interfacial tension data between the oil and NaCl-H<sub>2</sub>O solutions (1000 ppm) containing 0.01, 0.03, and 0.05 wt.% of SiO<sub>2</sub> (a) or TiO<sub>2</sub> (b) NPs.

used for the Zeta potential analysis under ambient condition.

The stability of solutions varies with the value of Zeta potential. If the absolute value of Zeta potential is between 0-10 mV, the solution is unstable. Otherwise, the solution is semi-stable when the absolute value of Zeta potential is

between 20-30 mV, and the solution is extremely stable when the absolute value of Zeta potential is between 30-60 mV [25-31]. Nano-saline solutions containing 0.05 wt.% of SiO<sub>2</sub> or TiO<sub>2</sub> NPs were stable due to the value of the Zeta potential that was higher than 30 mV. However, nano-saline solutions containing 0.07 wt.% of SiO<sub>2</sub> were semi-stable due to Zeta potential value that was less than 30 mV. It is worth mentioning that we could not measure the IFT of TiO<sub>2</sub>-saline solution at 0.07 wt.%, as it was an opaque solution. For this reason, the Zeta potential of TiO<sub>2</sub>-saline solution at 0.07 wt.%, was not measured. Therefore, the optimum concentration of SiO<sub>2</sub> NPs was considered 0.05 wt.%, based on the results of IFT measurements in various concentrations (0.01, 0.03, and 0.05 wt.%) and Zeta potential measurements. However, for TiO<sub>2</sub> NPs the optimum concentration could not be obtained; its suitable value for the IFT reduction assessed in this work was considered 0.05 wt.%.

Figure 5 shows the experimental interfacial tension data between the oil and CaSO<sub>4</sub>-H<sub>2</sub>O solutions (1000 ppm) containing 0.01, 0.03, 0.05, and 0.07 wt.% of SiO<sub>2</sub> NPs, and 0.01, 0.03, and 0.05 wt.% of TiO<sub>2</sub> NPs. According to our results, the interfacial tension, as the force holding the surface of a particular phase together, decreased with an increase in pressure, and caused an increase in concentration of NPs up to 0.05 wt.% in the CaSO<sub>4</sub>-H<sub>2</sub>O solutions. These observed interfacial tensions can arise from the two opposite effects of the nanoparticles: first, the depletion of the saline solution due to the adsorption of NPs on the particles interface, which leads to an increase in interfacial tension with changes in the particle content. Second, the

**Table 2.** Zeta Potential of SiO<sub>2</sub> Saline-nanofluid and TiO<sub>2</sub> Saline-nanofluid at Different Concentrations after the End of each Experiment

Nano-saline Solution	Zeta potential (mV)	Nano-saline solution	Zeta potential (mV)
SiO <sub>2</sub> -NaCl-nanofluid (0.05 wt.%)	-35.8	TiO <sub>2</sub> -NaCl-nanofluid (0.05 wt.%)	-35.4
SiO <sub>2</sub> -CaSO <sub>4</sub> -nanofluid (0.05 wt.%)	-30.2	TiO <sub>2</sub> -CaSO <sub>4</sub> -nanofluid (0.05 wt.%)	-41.3
SiO <sub>2</sub> -MgSO <sub>4</sub> -nanofluid (0.05 wt.%)	-31.6	TiO <sub>2</sub> -MgSO <sub>4</sub> -nanofluid (0.05 wt.%)	-31.5
SiO <sub>2</sub> -NaCl-nanofluid (0.07 wt.%)	-26.6	-	-
SiO <sub>2</sub> -CaSO <sub>4</sub> -nanofluid (0.07 wt.%)	-22.0	-	-
SiO <sub>2</sub> -MgSO <sub>4</sub> -nanofluid (0.07 wt.%)	-24.1	-	-

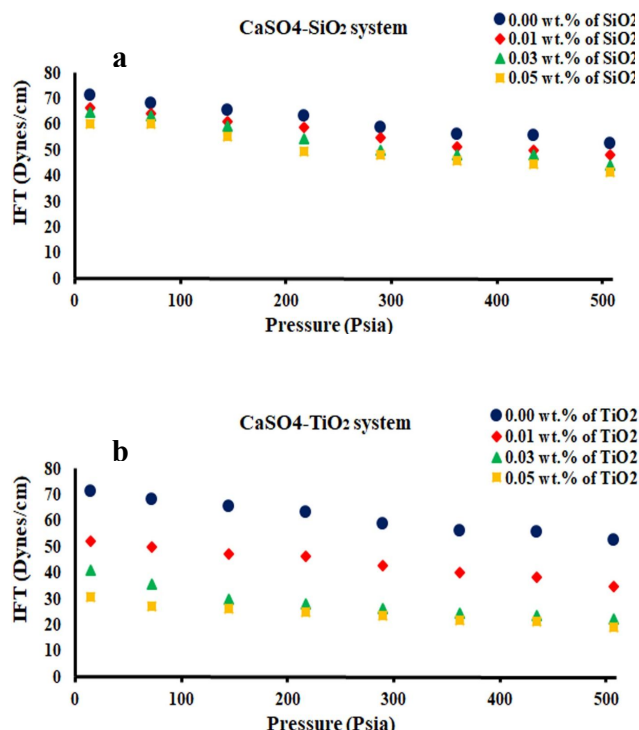


**Fig. 5.** Experimental interfacial tension data between the oil and CaSO<sub>4</sub>-H<sub>2</sub>O solutions (1000 ppm) containing 0.01, 0.03 and 0.05 wt.% of SiO<sub>2</sub> (a) or TiO<sub>2</sub> (b) NPs.

attachment of particles at the interfacial layers, which decreases the interfacial tension. Therefore, SiO<sub>2</sub> and/or attachment of particles at the interfacial layers, which decreases the interfacial tension. Therefore, SiO<sub>2</sub> and/or TiO<sub>2</sub> NPs play an important role in reducing the IFT in CaSO<sub>4</sub>-H<sub>2</sub>O solutions. Other researchers [32,33] have confirmed the reduction of IFT using NPs.

Figure 6 shows the experimental interfacial tension data between the oil and MgSO<sub>4</sub>-H<sub>2</sub>O solutions (1000 ppm) with the concentrations of 0.01, 0.03, 0.05, and 0.07 wt.% of SiO<sub>2</sub> NPs and 0.01, 0.03, and 0.05 wt.% of TiO<sub>2</sub> NPs. Results revealed that SiO<sub>2</sub> and/or TiO<sub>2</sub> NPs intensified the reduction of the oil interfacial tension. The reason for this decrease in IFT can be attributed to the increase in conductivity, the presence of active ions (charge effect) in the solution. Generally, conductivity of the nanofluids increases linearly with an increase in concentration. In addition, rising pressure and the concentration of NPs in the

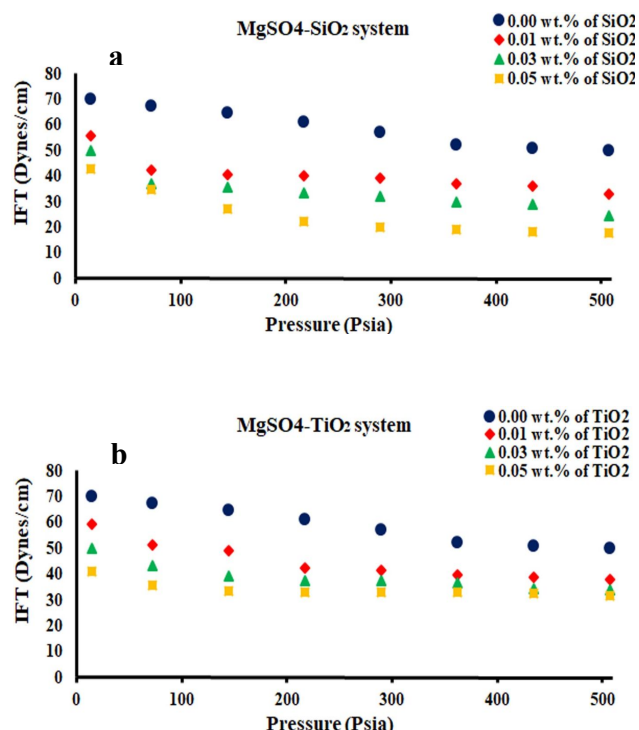


**Fig. 6.** Experimental interfacial tension data between the oil and MgSO<sub>4</sub>-H<sub>2</sub>O solutions (1000 ppm) containing 0.01, 0.03 and 0.05 wt.% of SiO<sub>2</sub> (a) or TiO<sub>2</sub> (b) NPs.

MgSO<sub>4</sub>-H<sub>2</sub>O solutions can directly affect the IFT reduction. This confirms that IFT is a function of pressure and the composition of each phase. IFT reduction using NPs has been acknowledged by other researchers in MgSO<sub>4</sub>-H<sub>2</sub>O solutions [33,34].

Figure 7 compares the ability of two different NPs (SiO<sub>2</sub>/TiO<sub>2</sub>) in reducing the IFT between the oil and different saline solutions at different pressures and different NPs concentrations. Results illustrated that surface active materials have a measurable effect on surface tension. Besides, SiO<sub>2</sub> NPs are more effective in decreasing the oil interfacial tension than TiO<sub>2</sub> NPs. Both physical and/or chemical properties of the adsorbent affect the IFT reduction. The size of NPs plays an important role in their physical properties, as higher repulsion forces are contributed with smaller NPs size. On the other hand, the ultra-small size of NPs causes agglomeration phenomenon. In this study, the size of SiO<sub>2</sub> or TiO<sub>2</sub> NPs was considered

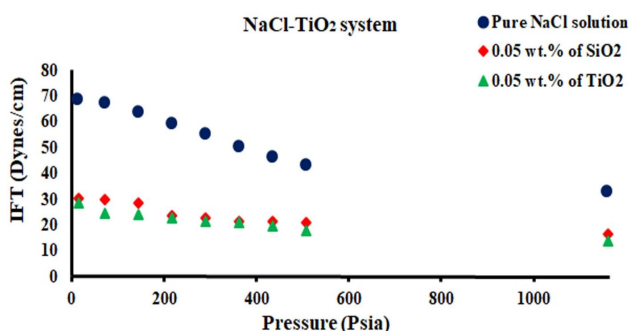


**Fig. 7.** Comparison results between two different NPs (SiO<sub>2</sub> /TiO<sub>2</sub>) in reducing the IFT between the oil and different saline solutions at different pressures and NPs concentrations.

20-30 nm. Since adsorbents were similar in shape and size, the appeared difference between SiO<sub>2</sub> and TiO<sub>2</sub> can be attributed to chemical properties of NPs such as the available functional groups in their structures. The more important difference between Ti-O and Si-O bonds is that silicon is more electronegative than titanium, ( $\chi_{\text{Ti}} = 1.54$ ,  $\chi_{\text{Si}} = 1.90$ ), which causes the formation of more chemical bonds between Si and available mineral ions leading to formation of a thicker nanolayer, as nanofilm, on the solid surface. However, immethodical increase in the NPs concentration can decrease the porosity and permeability of the reservoir rock because of NPs' agglomeration and high NPs deposition on the rock surface [36].

In this study, the effect of 21 different nano saline solutions on the oil IFT was examined. In all experiments, the IFT reduction in the presence of the NPs was more than that in the absence of the NPs. Although all of the low salinity solutions could reduce IFT, the effect of divalent cations was more than that of monovalent ones. Increasing the pressure and NPs concentration had desirable effects on the oil IFT reduction. SiO<sub>2</sub> NPs was more efficient than TiO<sub>2</sub> NPs in reducing oil IFT. The Zeta potential results indicated that TiO<sub>2</sub>-saline solutions were stable up to 0.05 wt.%, and also confirmed that the optimum NPs concentration for SiO<sub>2</sub>-saline solutions assessed in this work was 0.05 wt.%.

## CONCLUSIONS

In this study, several saline solutions (NaCl; CaSO<sub>4</sub>;

and/or the MgSO<sub>4</sub>) containing SiO<sub>2</sub> and/or TiO<sub>2</sub> NPs were prepared. The interfacial tension was measured between the oil and the saline solutions containing NPs with the concentration range from 0.01 to 0.07 wt.% for SiO<sub>2</sub> and from 0.01 to 0.05 for TiO<sub>2</sub>. The measurmnets were performed at low and intermediate pressures using a homemade high-pressure IFT device. Results revealed that the addition of 0.05 wt.% of the SiO<sub>2</sub> or TiO<sub>2</sub> NPs to the saline solution decreased the oil interfacial tension by a factor of 63.95% and 63.46%, respectively, and therefore increased the oil recovery factor. Additionally, an increase in pressure and NPs concentration caused a decrease in the oil IFT.

## ACKNOWLEDGMENTS

The authors are grateful to the Shiraz University and Enhanced Gas Condensate Recovery Research Group for supporting this research.

## REFERENCES

- [1] Elkady, M., Application of nanotechnology in EOR, polymer-nano flooding the nearest future of chemical EOR. *In SPE Annual Technical Conference and Exhibition*. **2016**. Society of Petroleum Engineers.
- [2] Amanullah, M.; Al-Arfaj, M. K.; Al-Abdullatif, Z. A., Preliminary test results of nano-based drilling fluids for oil and gas field application. *In SPE/IADC Drilling Conference and Exhibition*. **2011**. Society of Petroleum Engineers.
- [3] Taghizadeh, F.; Mokhtarani, B.; Zadmand, R.; Jalali, M. R., Highly selective CO<sub>2</sub> uptake in calix [4] arene compounds immobilized on silica gel. *Chem. Eng. J.*, **2020**, *417*, 128115. <https://doi.org/10.1016/j.cej.2020.128115>.
- [4] Moradi, B.; Pourafshary, P.; Jalali Farahani, F.; Mohammadi, M.; Emadi, M. A., Application of SiO<sub>2</sub> nano particles to improve the performance of water alternating gas EOR process. *In SPE Oil & Gas India Conference and Exhibition*. **2015**. Society of Petroleum Engineers.
- [5] Tarek, M., Investigating nano-fluid mixture effects to enhance oil recovery. *In SPE Annual Technical*

- Conference and Exhibition. **2015**. Society of Petroleum Engineers.
- [6] Salem Ragab, A. M.; Hannora, A. E., A comparative investigation of nano particle effects for improved oil recovery-experimental work. In *SPE Kuwait oil and Gas Show and Conference*. **2015**. Society of Petroleum Engineers.
- [7] Zandahvifard, M. J.; Elhambakhsh, A.; Ghasemi, M. N.; Esmailzadeh, F.; Parsaei, R.; Keshavarz, P.; Wang, X., Effect of modified Fe<sub>3</sub>O<sub>4</sub> magnetic NPs on the absorption capacity of CO<sub>2</sub> in water, wettability alteration of carbonate rock surface, and water-oil interfacial tension for oilfield applications. *I & EC Research*, **2021**, *60*, 3421-3434,, <https://doi.org/10.1021/acs.iecr.0c04857>.
- [8] Kong, X.; Ohadi, M., Applications of micro and nano technologies in the oil and gas industry-overview of the recent progress. In *Abu Dhabi International Petroleum Exhibition and Conference*. **2010**. Society of Petroleum Engineers.
- [9] Qiu, F., The potential applications in heavy oil EOR with the nanoparticle and surfactant stabilized solvent-based emulsion. In *Canadian Unconventional Resources and International Petroleum Conference*. **2010**. Society of Petroleum Engineers.
- [10] Biyouki, A. A., In-situ upgrading of reservoir oils by in-situ preparation of NiO nanoparticles in thermal enhanced oil recovery processes. *Colloids Surf. A: Physicochem. Eng. Asp.*, **2017**, *520*, 289-300, <https://doi.org/10.1016/j.colsurfa.2017.01.089>.
- [11] Ranjbar, H.; Khosravi-Nikou, M. R.; Safiri, A.; Bovard, S.; Khazaei, A., Experimental and theoretical investigation on Nano-fluid surface tension. *J. Nat. Gas Sci. Eng.*, **2015**, *27*, 1806-1813, <https://doi.org/10.1016/j.jngse.2015.11.010>.
- [12] Amraei, A.; Fakhroueian, Z.; Bahramian, A., Influence of new SiO<sub>2</sub> nanofluids on surface wettability and interfacial tension behaviour between oil-water interface in EOR processes. *J. Nano Res.*, **2014**, *26*, 1-8, Trans Tech Publ. <https://doi.org/10.4028/www.scientific.net/JNanoR.26.1>.
- [13] Zaid, H. M., Effect of morphology of aluminium oxide nanoparticles on viscosity and interfacial tension (IFT) and the recovery efficiency in enhanced oil recovery (EOR). In *AIP Conference Proceedings*. **2014**. AIP.
- [14] Lager, A.; Webb, K. J.; Black, C. J. J.; Singleton, M.; Sorbie, K. S., Low salinity oil recovery-an experimental investigation. *Petrophysics*, **2008**, *49*, <https://doi.org/10.1016/B978-0-12-803188-9.00005-X>.
- [15] Alnarabiji, M. S., Nanofluid enhanced oil recovery using induced ZnO nanocrystals by electromagnetic energy: Viscosity increment. *Fuel*, **2018**, *233*, 632-643. <https://doi.org/10.1016/j.fuel.2018.06.068>.
- [16] Mokhtari, K.; Wagner, A. R., The pedestrian patterns dataset. arXiv preprint arXiv:2001.01816, **2020**.
- [17] Mokhtari, K.; Ayub, A.; Surendran, V.; Wanger, A. R., Pedestrian density based path recognition and risk prediction for autonomous vehicles. In *2020 29th IEEE International Conference on Robot and Human Interactive Communication (RO-MAN)*. **2020**. IEEE.
- [18] Ameri, A.; Esmailzadeh, F.; Mowla, D., Effect of brine on asphaltene precipitation at high pressures in oil reservoirs. *Pet. Chem.*, **2018**, *58*, 1076-1084, <https://doi.org/10.1134/S096554411810002X>.
- [19] Safaei, A.; Esmailzadeh, F.; Sardarian, A.; Mousavi, S. M.; Wang, X., Experimental investigation of wettability alteration of carbonate gas-condensate reservoirs from oil-wetting to gas-wetting using Fe<sub>3</sub>O<sub>4</sub> nanoparticles coated with poly (vinyl alcohol), (PVA) or hydroxyapatite (HAp). *J. Pet. Sci. Eng.*, **2019**, *184*, 106530, <https://doi.org/10.1016/j.petrol.2019.106530>.
- [20] Pereira, L. M.; Chapoy, A.; Burgass, R., Study of the impact of high temperatures and pressures on the equilibrium densities and interfacial tension of the carbon dioxide/water system. *J. Chem. Thermodyn.*, **2016**, *93*, 404-415, <https://doi.org/10.1016/j.jct.2015.05.005>.
- [21] Andreas, J.; Hauser, E.; Tucker, W., Boundary tension by pendant drops1. *J. Phys. Chem.*, **2002**, *42*, 1001-1019, DOI: <https://doi.org/10.1021/j100903a002>.
- [22] Rahmatmand, B.; Keshavarz, P.; Ayatollahi, S., Study of absorption enhancement of CO<sub>2</sub> by SiO<sub>2</sub>, Al<sub>2</sub>O<sub>3</sub>, CNT, and Fe<sub>3</sub>O<sub>4</sub> nanoparticles in water and amine solutions. *J. Chem Eng., Data*, **2016**, *61*, 1378-1387. <https://doi.org/10.1021/acs.jced.5b00442>.

- [23] Elhambakhsh, A.; Keshavarz, P., Effects of different amin-based core-shell magnetic NPs on CO<sub>2</sub> capture using NMP solution at high pressures. *J. Nat. Gas Sci. Eng.*, **2020**, *84*, 103645, <https://doi.org/10.1016/j.jngse.2020.103645>.
- [24] Elhambakhsh, A.; Keshavarz, P., Enhanced CO<sub>2</sub> capture efficiency applying amine-based nano magnetite/sulfinol-M nano solvents at high pressures. *Environ. Sci. Pollut. Res.*, **2021**, *28*, 3455-3464, <https://doi.org/10.1007/s11356-020-10756-6>.
- [25] Ali, N.; Teixeira, J. A.; Addali, A., A review on nanofluids: Fabrication, stability, and thermophysical properties. *J. Nanomater.*, **2018**, *2018*, 6978130, <https://doi.org/10.1155/2018/6978130>.
- [26] Elhambakhsh, A.; Zaeri, M. R.; Mehdipour, M.; Keshavarz, P., Synthesis of different modified magnetic nanoparticles for selective physical/chemical absorption of CO<sub>2</sub> in a bubble column reactor. *J. Environ. Chem. Eng.*, **2020**, *8*, 104195, <https://doi.org/10.1016/j.jece.2020.104195>.
- [27] Elhambakhsh, A.; Keshavarz, P., Investigation of carbon dioxide absorption using different functionalized Fe<sub>3</sub>O<sub>4</sub> magnetic nanoparticles. *Energy Fuels*, **2020**, *34*, 7198-7208, <https://doi.org/10.1021/acs.energyfuels.0c00234>.
- [28] Shadanfar, H.; Elhambakhsh, A.; Keshavarz, P., Air dehumidification using various TEG based nano solvents in hollow fiber membrane contactors. *Heat Mass Transf.*, **2021**, *57*, 1623-1631, <https://doi.org/10.1007/s00231-021-03057-2>.
- [29] Elhambakhsh, A.; Ghanaatian, A.; Keshavarz, P., Glutamine functionalized iron oxide nanoparticles for high-performance carbon dioxide absorption. *J. Nat. Gas Sci. Eng.*, **2021**, *96*, 10408, <https://doi.org/10.1016/j.jngse.2021.104081>.
- [30] Mehdipour, M.; Elhambakhsh, A.; Keshavarz, P.; Rahimpour, M. R., CO<sub>2</sub> Separation by rotating liquid sheet contactor: A novel procedure to improve mass transfer characterization. *Chem. Eng. Res. Des.*, **2021**, *172*, 120-126., <https://doi.org/10.1016/j.cherd.2021.06.008>
- [31] Elhambakhsh, A.; Heidari, S.; Keshavarz, P., Experimental study of CO<sub>2</sub> absorption by Fe<sub>2</sub>O<sub>3</sub>@glutamine/NMP nanofluid. *Environ. Sci Pollut. Res.*, **2021**, <https://doi.org/10.1007/s11356-021-15650-3>.
- [32] Han, P., Mechanistic understanding of water-rock interactions during high-salinity water-flooding of carbonate reservoirs, **2016**. *Missouri University of Science and Technology*.
- [33] Freyer, D.; Voigt, W., Crystallization and phase stability of CaSO<sub>4</sub> and CaSO<sub>4</sub>-based salts. *Monatsh. Chem.*, **2003**, *134*, 693-719. <https://doi.org/10.1007/s00706-003-0590-3>.
- [34] Cheraghian, G.; Rostami, S.; Afrand, M., Nanotechnology in enhanced oil recovery. *Processes*, **2020**, *8*, 1073. <https://doi.org/10.3390/pr8091073>.
- [35] Kamal, M.; Adewunmi, A.; Sultan, A.; Al-Hamad, M.; Mehmood, U., Recent advances in nanoparticles enhanced oil recovery: Rheology, interfacial tension, oil recovery, and wettability alteration., *Nanomaters*, **2017**, *2017*, 2473175 <https://doi.org/10.1155/2017/2473175>.
- [36] Zhe, Z.; Yuxiu, A., Nanotechnology for the oil and gas industry-an overview of recent progress. *Nanotechnology Reviews*, **2018**, *7*, 341-353. <https://doi.org/10.1515/ntrev-2018-0061>.